

Development of a Working Model of the Active Site in Bovine Lens Leucine Aminopeptidase: A Density Functional Investigation

Stefan Erhardt and Jennie Weston^{*[a]}

Dedicated to Prof. Dr. Ernst Anders
on the occasion of his 60th birthday

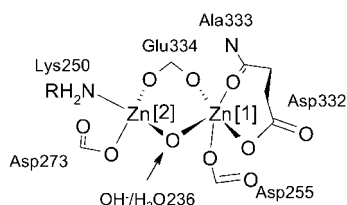
KEYWORDS:

aminopeptidases · density functional calculations · enzyme models · metalloenzymes

Leucine aminopeptidases (LAPs) are known to play a critical role in the degradation of proteins and the metabolism of biologically active peptides.^[1] These cytosolic exopeptidases are ubiquitous in nature and are present not only in animals, but also in plants and bacteria. Extensive kinetic and crystallographic investigations on the variant isolated from bovine lens^[2–4] (*b*LAP; EC 3.4.11.1) have made this enzyme currently one of the best-studied dizinc peptidases.

High-resolution X-ray crystal structures have been determined not only for the native *b*LAP^[5, 6] but also for several inhibitor complexes, for example, bestatin,^[5, 7] amastatin,^[8] L-leucinal,^[6] and L-leucinephosphonic acid.^[9] These inhibitor complexes are believed to be transition state analogues and current mechanistic conceptions for LAPs have been derived from their binding modes.^[6, 9, 10]

In the native enzyme, two zinc ions are necessary in order for the enzyme to be able to carry out the hydrolysis at the N terminus of the peptide. The two zinc atoms do not occupy identical coordination sites (see Scheme 1); this has led to the designation of zinc site 1, Zn[1], and zinc site 2, Zn[2], in the literature. Zn[1] can be replaced with magnesium, manganese, or cobalt ions.^[2, 11] However, Zn[2] is tightly bonded and a cobalt ion can occupy its place only if zinc is not present in the culture medium when the enzyme is expressed.^[12]



Scheme 1. Schematic representation of the active site of *b*LAP as taken from the X-ray crystal structure analysis.^[5, 6]

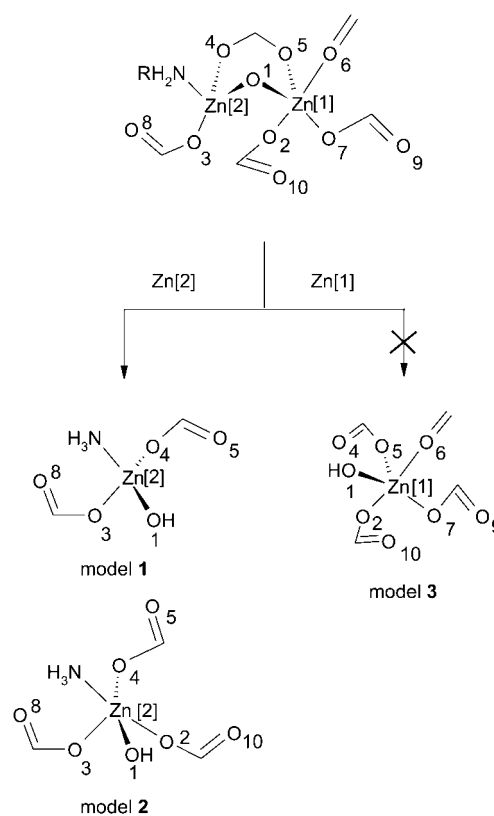
[a] J. Weston, S. Erhardt

Institut für Organische Chemie und Makromolekulare Chemie
der Friedrich-Schiller-Universität
Humboldtstrasse 10, 07743 Jena (Germany)
Fax: (+49) 3641-9-48212
E-mail: c9weje@rz.uni-jena.de

We took the X-ray crystal structure of the native enzyme as a starting point,^[5, 6] dissected its active site, and examined it extensively. The goal of this study was to find a working model of the active site which accurately reproduces the structural and electronic properties of the bimetallic center, but which is small enough to allow us to use it for detailed mechanistic density functional studies on the mode of action of *b*LAP.

Binuclear and mononuclear models were constructed by using retrosynthetic analysis of the X-ray crystal structure of the active site of *b*LAP (Scheme 2). The amino acid residues in the first coordination sphere of each metal ion were approximated with smaller (computationally amenable) ligands that were selected not only to structurally resemble the native site, but also to ensure that the resulting complexes remain as electroneutral as possible.

Tetrahedrally coordinated Zn[2] site: Calculations on a simplified model for the Zn[2] site (model 1 in Scheme 2 and Figure 1) show that this complex (total charge of -1) is energetically stable. Comparison of the structural data of model



Scheme 2. Simple monometallic models.

1 with the crystallographic data of the enzyme shows a relatively good agreement between the calculated Zn[2]–ligand bond lengths and the X-ray data of the Zn[2] coordination site in the enzyme (Table 1). The Zn[2]–O1 distance is approximately 0.05 Å shorter than that observed in the free enzyme because of the missing bridge to the Zn[1] ion. The only other Zn[2]–ligand bond length which deviates significantly (by more than about 0.02 Å) from the X-ray data is the Zn–O3 bond length (0.07 Å too

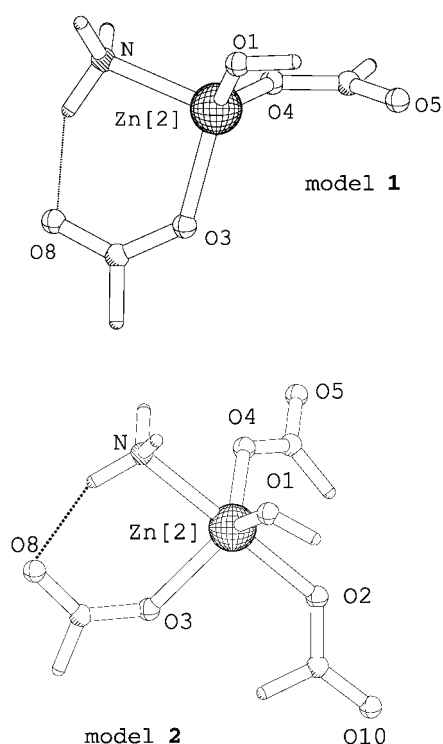


Figure 1. Models 1 and 2 of the Zn[2] site in bLAP. Calculated at the B3LYP/6-311 + G(d,p) level of theory.

Table 1. Selected bond lengths (Å) and angles (°), and the dihedral angle (°), calculated at the B3LYP/6-311 + G(d,p) level of theory, for the model complexes 1 and 2 as compared to X-ray data^[5, 6] for the active site in the native enzyme.

	Model 1	Model 2	X-ray data
Zn[2]–O1	1.894	1.967	1.951
Zn[2]–O2	–	2.114	2.595
Zn[2]–O3	2.047	2.185	1.981
Zn[2]–O4	2.007	2.102	2.015
Zn[2]–N	2.146	2.225	2.174
N–O8	2.847	2.937	3.097
N–Zn[2]–O1	104.8	85.1	101.8
N–Zn[2]–O2	–	176.5	173.4
N–Zn[2]–O3	97.2	81.4	98.6
N–Zn[2]–O4	95.8	87.1	100.8
O1–Zn[2]–O3	118.9	121.2	143.3
O1–Zn[2]–O4	126.3	121.1	104.4
O3–Zn[2]–O4–O1	–147.4	161.5	–153.6

long in the model). The calculated bond angles (with the exception of the O1–Zn–O angles) are also in relatively good agreement with the native enzyme.

The ammonia ligand in model 1 exhibits a hydrogen bond to O8 which stabilizes the Zn–N contact. If the carboxylate group is rotated by 180° about the C–O3 bond axis or replaced with a hydroxide group (which removes the hydrogen bond in both cases), an unstable complex results. Optimization of such complexes results invariably in the immediate elimination of NH₃ and the formation of a trigonal-planar Zn species.

The Zn[2] site is clearly tetrahedral in the native enzyme. However, we expect its coordination sphere to be very flexible

since an extended ab initio study on hydrated Zn²⁺ ions showed that varying the local environment of the zinc ion (coordination numbers from four to six) costs very little energy (only about 1 kcal mol^{–1}).^[13] Addition of a further carboxylate ion to the optimized structure of model 1 results in an energetically stable trigonal-bipyramidal complex (model 2). The additional negative charge in the system causes a slight lengthening of all Zn[2]–ligand bonds but, on the whole, this arrangement agrees surprisingly well with the X-ray data. In fact, the carboxylate group of Asp255 (O2 in the calculation) is only 2.595 Å away from Zn[2] in the enzyme.^[5, 6] A slight displacement (ca. 0.5 Å) of this rather flexible amino acid residue could easily result in an extension of the coordination sphere of Zn[2].

Trigonal-bipyramidal coordinated Zn[1] site: We encountered serious problems in finding a computational model for the Zn[1] site. In the X-ray crystal structure, the carbonyl unit (O6) of Ala333 is 2.118 Å away from Zn[1]. All attempts to model this Zn[1]–O6 contact failed. (One example is model 3 in Scheme 2 which has a total charge of –2.) It proved impossible to persuade the carbonyl oxygen to remain inside of the first coordination sphere of Zn[1]. To reduce the negative charge, the carbonate groups/hydroxide ions were replaced with water molecules in all possible combinations but such changes did not help; the trigonal-bipyramidal coordination remained unstable. An extensive study of the coordination sphere of a zinc ion surrounded by hydroxide groups and water molecules^[14] supports our findings. It is unlikely that a neutral ligand can bind to the zinc ion if all the existing binding atoms are “hard”, e.g. oxygen, and if there are negatively charged ligands present.^[14] It is a very interesting fact that nature does exactly this in the Zn[1] site of bLAP.

Bimetallic models: We assumed that the unusual trigonal-pyramidal coordination on Zn[1] in bLAP is mainly due to steric effects and not electrostatic and/or electronic interactions and extended model 1 to build a bimetallic complex. This complex included the important backbone atoms around Zn[1] which link the Asp(332), Ala333 and Glu334 together. Optimization led to model 4 (a minimum on the hypersurface) in which a five-coordinated Zn[1] is present (Figure 2 and Table 2). There are two structural problems present in addition to the size of model 4 (it is simply too large to use for extended mechanistic studies). In the model, O2 bridges both Zn ions; in the enzyme Zn[2] has only a weak electrostatic contact to O2. Steric effects are not adequately represented in model 4 because of the simplicity of the included backbone, and the almost perfect trigonal-bipyramidal coordination at Zn[1] in the X-ray crystal structure of bLAP mutates into a distorted quadratic-pyramid geometry in the optimized structure. Still, the carboxylic oxygen O6 remains coordinated (O6–Zn[1] bond length: 2.108 Å), a definite indication that the backbone is indeed responsible for sustaining the unusual coordination at Zn[1]. A network of hydrogen bonds holds the carbonyl group inside of the Zn[1] coordination sphere (Figure 2). All of the other O–Zn[1] bond lengths are in good agreement with the X-ray data except for the O5–Zn[1] length which is slightly too long. This is caused by a strong hydrogen bond between O5 and the amine group in the peptide linking Glu334 and Ala333. This interaction is also present in the

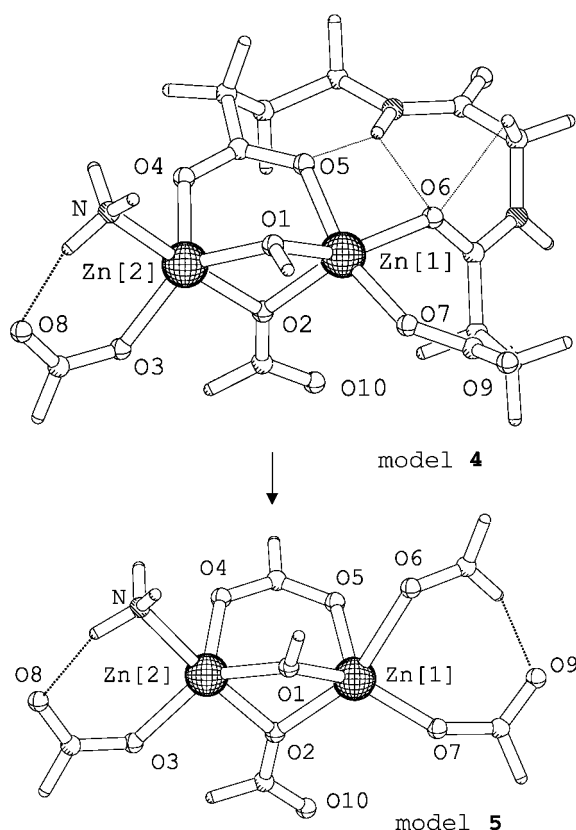


Figure 2. Development of a working model for the active site of bILAP. Calculated at the B3LYP/lan12dz level of theory.

Table 2. Selected bond lengths (Å) and angles (°), and the dihedral angles (°), calculated at the B3LYP/lan12dz level of theory, for the model complexes 4 and 5 as compared to X-ray data^[5, 6] for the active site in the native enzyme.

	Model 4	Model 5	X-ray data
Zn[1]–O1	2.007	1.998	2.013
Zn[1]–O2	2.066	2.074	2.123
Zn[1]–O5	2.172	2.078	2.022
Zn[1]–O6	2.108	2.457	2.118
Zn[1]–O7	1.999	1.951	1.983
Zn[2]–O1	2.020	2.013	1.951
Zn[2]–O2	2.167	2.113	2.595
Zn[2]–O3	2.038	2.041	1.981
Zn[2]–O4	2.082	2.122	2.015
Zn[2]–N1	2.166	2.182	2.174
O6–Zn[1]–O1	149.9	81.9	96.8
O6–Zn[1]–O2	123.4	157.1	178.2
O6–Zn[1]–O5	76.1	80.6	84.0
O6–Zn[1]–O7	86.2	90.2	85.2
N1–Zn[2]–O1	98.4	101.0	101.8
N1–Zn[2]–O2	177.0	174.6	173.4
N1–Zn[2]–O3	92.9	91.9	98.6
N1–Zn[2]–O4	89.6	86.5	100.8
O7–Zn[1]–O5–O1	–139.2	–163.4	–175.1
O3–Zn[2]–O4–O1	–168.4	–169.4	–153.6

enzyme, but is obviously stronger in model 4. The absence of both steric effects and a dielectric field probably cause the hydrogen-bond strength to be slightly overestimated in the model.

We succeeded in cutting away the backbone again in model 5. We realized that stabilizing hydrogen bonds are responsible for holding the carbonyl group in place and used formaldehyde to represent the carbonylic peptide moiety. We could generate a hydrogen bond to the carbonyl group by rotating the carbonate group O7CO9 that was used to model the Asp332 about the C–O7 bond axis. The stabilization provided by the backbone in model 4 was thereby replaced. The carbonyl group was held within the coordination sphere of Zn[1] by an H–O9 interaction, similar to the interaction which fixes the ammonia at the Zn[2] site (Figure 2). Interestingly enough, the distorted quadratipyramidal geometry is removed along with the backbone and the Zn[1] center takes on a trigonal-bipyramidal structure with O6 at an axial position, which is the correct coordination geometry according to the X-ray crystal structure. The largest deviation between the X-ray crystal structure and model 5 is that O2 bridges both Zn ions, although the calculated O2–Zn[2] bond (2.113 Å) is marginally longer than the O2–Zn[1] bond length (2.074 Å). In 5, the hydroxide ion evenly bridges the two zinc ions. (A hydroxide group is definitely present rather than water, since we could not locate any stable hydrated dizinc structures on the calculated hypersurface (B3LYP/lan12dz level of theory). Considering the well known enhancement of the acidity of H₂O in the first coordination sphere of a zinc ion,^[15] this is not surprising.) All other geometry parameters compare very well with the X-ray data and, within the accuracy of the experimental data, model 5 reproduces the structural geometry of the active site quite satisfactorily.

This working model is small enough to make extended mechanistic studies possible while accurately reproducing the structural and electrostatic properties of the first coordination sphere around the two Zn ions in the bimetallic active site of the enzyme. We showed that it is not necessary to include the backbone in the model in order to obtain the unusual trigonal-bipyramidal coordination geometry on Zn[1]. A carefully selected, induced hydrogen bond can replace the backbone since its purpose is apparently to “glue” the carbonyl function (O6) of Ala 333 in place. The major problem with the model is that O2 bridges the two zinc ions; in the X-ray crystal structure, only a very weak electrostatic contact between Zn[2] and O2 is present. Whether or not O2 (Asp 255) is important for substrate binding/hydrolysis is not known. Only detailed mechanistic calculations will reveal its role in the hydrolysis process.

The docking mechanism of a peptide chain onto the active site (modelled by 5) and the following hydrolysis of the N-terminal amino acid is currently the topic of investigation and will be reported on in a future article.

Computational Details

All calculations reported in this article were performed by using the Gaussian98^[16] program package with the gradient-corrected B3LYP^[17] density functional. Default convergence criteria were used for all calculations. Pople's 6-311 + G(d,p) basis set was employed for the smaller monozinc species. The large number of heavy atoms in the binuclear complexes, and especially the presence of two Zn atoms, limited the calculation on the larger bimetallic models to the

lan12dz basis set developed by Hay and Wadt (this basis set employs an effective core potential on zinc). Both basis sets were used as implemented in the standard basis set library of Gaussian98. The lan12dz basis set not only gave structural data that were directly comparable to the larger all-electron basis, but also eliminated self-consistent-field (SCF) convergence problems which occurred when the 6-311 + G(d,p) basis set was used for the larger systems. Atomic charges and hyperconjugative interaction energies were obtained by using the natural bond orbital analysis of Reed et al.^[18] as implemented in Gaussian98.

- [1] a) H. Umeweza, *Recent Results Cancer Res.* **1980**, *75*, 115; b) A. Taylor, *FASEB J.* **1993**, *7*, 290; c) A. Taylor, *Trends Biochem. Sci.* **1993**, *18*, 167.
- [2] F. H. Carpenter, J. M. Vahl, *J. Biol. Chem.* **1973**, *248*, 294.
- [3] a) F. H. Carpenter, K. Y. Harrington, *J. Biol. Chem.* **1972**, *247*, 5580; b) S. W. Melbye, F. H. Carpenter, *J. Biol. Chem.* **1971**, *246*, 2459.
- [4] a) N. Sträter, W. N. Lipscomb, *Chem. Rev.* **1996**, *96*, 2375; b) N. Sträter, W. N. Lipscomb, T. Klabunde, B. Krebs, *Angew. Chem.* **1996**, *108*, 2158; *Angew. Chem. Int. Ed. Engl.* **1996**, *35*, 2024; c) H. Kim, W. N. Lipscomb, *Adv. Enzymol.* **1994**, *68*, 153.
- [5] a) S. K. Burley, P. R. David, R. M. Sweet, A. Taylor, W. N. Lipscomb, *J. Mol. Biol.* **1992**, *224*, 113.
- [6] N. Sträter, W. N. Lipscomb, *Biochemistry* **1995**, *34*, 14792.
- [7] S. K. Burley, P. R. David, A. Taylor, W. N. Lipscomb, *Proc. Natl. Acad. Sci. USA* **1990**, *87*, 6878.
- [8] A. Taylor, C. Z. Peltier, F. J. Torre, *Biochemistry* **1993**, *32*, 784.
- [9] N. Sträter, W. N. Lipscomb, *Biochemistry* **1995**, *34*, 9200.
- [10] N. Sträter, L. Sun, E. R. Kantrowitz, W. N. Lipscomb, *Proc. Natl. Acad. Sci. USA* **1999**, *96*, 11151.
- [11] a) H. Kim, W. N. Lipscomb, *Biochemistry* **1993**, *32*, 8465; b) H. Kim, W. N. Lipscomb, *Proc. Natl. Acad. Sci. USA* **1993**, *90*, 5006.
- [12] a) P. Allen, A. H. Yamada, F. H. Carpenter, *Biochemistry* **1983**, *22*, 3778; b) G. A. Thompson, F. H. Carpenter, *J. Biol. Chem.* **1976**, *251*, 1618.
- [13] C. W. Bock, A. K. Katz, J. P. Glusker, *J. Am. Chem. Soc.* **1995**, *117*, 3754.
- [14] G. Tiraboschi, N. Gresh, C. Giessner-Prettre, L. G. Pedersen, D. W. Deerfield, *J. Comp. Chem.* **2000**, *21*, 1011.
- [15] M. Mauksch, M. Bräuer, J. Weston, E. Anders, *ChemBioChem* **2001**, *2*, 190–198, and references cited therein.
- [16] Gaussian98 (Revision A.7), M. J. Frisch, G. W. Trucks, H. B. Schlegel, G. E. Scuseria, M. A. Robb, J. R. Cheeseman, V. G. Zakrzewski, J. A. Montgomery, R. E. Stratmann, J. C. Burant, S. Dapprich, J. M. Millam, A. D. Daniels, K. N. Kudin, M. C. Strain, O. Farkas, J. Tomasi, V. Barone, M. Cossi, R. Cammi, B. Mennucci, C. Pomelli, C. Adamo, S. Clifford, J. Ochterski, G. A. Petersson, P. Y. Ayala, Q. Cui, K. Morokuma, D. K. Malick, A. D. Rabuck, K. Raghavachari, J. B. Foresman, J. Cioslowski, J. V. Ortiz, B. B. Stefanov, G. Liu, A. Liashenko, P. Piskorz, I. Komaromi, R. Gomperts, R. L. Martin, D. J. Fox, T. Keith, M. A. Al-Laham, C. Y. Peng, A. Nanayakkara, C. Gonzalez, M. Challacombe, P. M. W. Gill, B. G. Johnson, W. Chen, M. W. Wong, J. L. Andres, M. Head-Gordon, E. S. Replogle, J. A. Pople, Gaussian, Inc., Pittsburgh, PA, **1998**.
- [17] a) A. D. Becke, *J. Chem. Phys.* **1993**, *98*, 1372; A. D. Becke, *J. Chem. Phys.* **1993**, *98*, 5648; b) C. Lee, W. Yang, R. G. Parr, *Phys. Rev. B* **1988**, *37*, 785; c) A. D. Becke, *Phys. Rev. A* **1988**, *38*, 3098.
- [18] A. E. Reed, R. B. Weinstock, F. Weinhold, *J. Chem. Phys.* **1985**, *83*, 735.

Received: July 16, 2001 [Z266]

Breakdown of Chlorophyll: Electrochemical Bilin Reduction Provides Synthetic Access to Fluorescent Chlorophyll Catabolites

Michael Oberhuber and Bernhard Kräutler*^[a]

KEYWORDS:

catabolite · chlorophyll · electrochemistry · enzyme catalysis · tetrapyrrole

Chlorophyll catabolites from plants have long remained undiscovered, and chlorophyll breakdown was elusive until about ten years ago.^[1,2] In contrast to all earlier expectations, the degradation of chlorophylls in senescent vascular plants rapidly progresses to colorless chlorophyll catabolites.^[1,3] Trace amounts of fluorescent compounds were detectable as intermediates in the breakdown of chlorophyll to the colorless catabolites.^[4] Minute samples of the two fluorescent chlorophyll catabolites (FCCs) **2a**^[5] and **2b**^[6] could be prepared with active enzyme extracts from pheophorbide a (1). The FCCs **2a** and **2b** are epimeric at their C(1) centers^[7] and are identified as the "primary" FCCs (pFCCs) of the two known (stereodivergent) paths of chlorophyll catabolism in higher plants (Scheme 1).^[8]

Enzymatic conversion of **1** to pFCCs requires pheophorbide a oxygenase (PaO), which oxygenates **1** to the elusive red chlorophyll catabolite (**3**, RCC), and RCC reductase (RCCR), which acts jointly with PaO to reduce RCC to one of the two epimeric pFCCs.^[3,9,10] Two types of RCCRs have thus evolved in higher plants^[8] which have no cofactor, but use reduced ferredoxin.^[10] The enzymatic reduction of RCC may therefore occur by one-electron steps.

We have set out to find an efficient preparative route to pFCCs by means of a non-enzymatic synthesis, and to specifically examine, for this purpose, the capacity of an electrochemical reduction of RCC (**3**).^[11] Herein we report on electro-synthetic studies, which have resulted in a preparative route to both epimeric lines of fluorescent chlorophyll catabolites. For practical reasons (stability problems encountered with the pFCC's **2a/2b**) the work was carried out with RCC methyl ester **4**.^[11] The reduction of **4** to the methyl esters of the two epimeric pFCCs (**5a** and **5b**; Scheme 2) was achieved by electrolysis in a two compartment cell: a deoxygenated solution of **4** in MeOH was electrochemically reduced at an Hg electrode at –1.3 V versus a 0.1 normal calomel electrode (NCE) reference.^[12] The reaction mixture was analyzed and purified by HPLC (see Figure 1 and Scheme 2). Four homogeneous fractions (**5a'** (ca. 1%), **5a** (12%),

[a] Prof. Dr. B. Kräutler, Mag. M. Oberhuber
Institute of Organic Chemistry
University of Innsbruck
Innrain 52a, 6020 Innsbruck (Austria)
Fax: (+43) 512-507-2892
E-mail: bernhard.kraeutler@uibk.ac.at